Radiotherapy and Oncology 200 (2024) 110475

Contents lists available at ScienceDirect

Radiotherapy and Oncology

journal homepage: www.thegreenjournal.com

Original Article

Talazoparib enhances resection at DSBs and renders HR-proficient cancer cells susceptible to Polθ inhibition

Xixi Lin [a,b], Aashish Soni [a,b,*], Razan Hessenow [c], Yanjie Sun [b,c], Emil Mladenov [a,b], Maja Guberina [d,e], Martin Stuschke [a,d,e], George Iliakis [a,b,*]

[a] Division of Experimental Radiation Biology, Department of Radiation Therapy, University Hospital Essen, University of Duisburg-Essen, 45147, Essen, Germany
[b] Institute of Medical Radiation Biology, University Hospital Essen, University of Duisburg-Essen, 45147, Essen, Germany
[c] West German Proton Therapy Center Essen (WPE), University of Duisburg-Essen, 45147, Essen, Germany
[d] Department of Radiation Therapy, West German Cancer Center, University Hospital Essen, University Duisburg-Essen, 45147, Essen, Germany
[e] German Cancer Consortium (DKTK), Partner Site University Hospital Essen, German Cancer Research Center (DKFZ), 45147, Essen, Germany

ARTICLE INFO

Keywords:
PARP inhibitors
BMN673
Talazoparib
Novobiocin
ART558
Homologous recombination
Radiotherapy
Cancer
DNA polymerase theta
DNA double strand breaks

ABSTRACT

Background and purpose: The PARP inhibitor (PARPi), Talazoparib (BMN673), effectively and specifically radiosensitizes cancer cells. Radiosensitization is mediated by a shift in the repair of ionizing radiation (IR)-induced DNA double-strand breaks (DSBs) toward PARP1-independent, alternative end-joining (alt-EJ). DNA polymerase theta (Polθ) is a key component of this PARP1-independent alt-EJ pathway and we show here that its inhibition can further radiosensitize talazoparib-treated cells. The purpose of the present work is to explore mechanisms and dynamics underpinning enhanced talazoparib radiosensitization by Polθ inhibitors in HR-proficient cancer cells.

Methods and Materials: Radiosensitization to PARPis, talazoparib, olaparib, rucaparib and veliparib was assessed by clonogenic survival. Polθ-proficient and −deficient cells were treated with PARPis and/or with the Polθ inhibitors ART558 or novobiocin. The role of DNA end-resection was studied by down-regulating CtIP and MRE11 expression using siRNAs. DSB repair was assessed by scoring γH2AX foci. The formation of chromosomal abnormalities was assessed as evidence of alt-EJ function using G_2-specific cytogenetic analysis.

Results: Talazoparib exerted pronounced radiosensitization that varied among the tested cancer cell lines; however, radiosensitization was undetectable in normal cells. Other commonly used PARPis, olaparib, veliparib, or rucaparib were ineffective radiosensitizers under our experimental conditions. Although genetic ablation or pharmacological inhibition of Polθ only mildly radiosensitized cancer cells, talazoparib-treated cells were markedly further radiosensitized. Mechanistically, talazoparib shunted DSBs to Polθ-dependent alt-EJ by enhancing DNA end-resection in a CtIP- and MRE11-dependent manner – an effect detectable at low, but not high IR doses. Chromosomal translocation analysis in talazoparib-treated cells exposed to Polθ inhibitors suggested that PARP1- and Polθ-dependent alt-EJ pathways may complement, but also back up each other.

Conclusion: We propose that talazoparib promotes low-dose, CtIP/MRE11-dependent resection and increases the reliance of irradiated HR-proficient cancer cells, on Polθ-mediated alt-EJ. The combination of Polθ inhibitors with talazoparib suppresses this option and causes further radiosensitization. The results suggest that Polθ inhibition may be exploited to maximize talazoparib radiosensitization of HR-proficient tumors in the clinic.

Introduction

Targeting tumors defective in BRCA1 or BRCA2, two central proteins of homologous recombination repair (HR), with poly-ADP-ribose polymerase (PARP) inhibitors is a striking example of precision oncology harnessing the concept of synthetic lethality [1–6]. Indeed, it is the first molecular-targeted therapy approved for this group of diseases [3]. HR removes replication-associated DSBs generated in cells treated with PARP inhibitors (PARPis), and when HR is defective, synthetically lethal effects impair their repair, eventually causing cell death. It is proposed [6] that PARP inhibition at base-excision repair sites, traps the protein onto DNA repair intermediates that obstruct replication forks and

* Corresponding authors.
E-mail addresses: aashish.soni@uk-essen.de (A. Soni), georg.iliakis@uk-essen.de (G. Iliakis).

https://doi.org/10.1016/j.radonc.2024.110475
Received 19 December 2023; Received in revised form 2 July 2024; Accepted 12 August 2024
Available online 13 August 2024

generate structures that are normally resolved by BRCA-dependent HR [7–9].

The mechanism of trapping has been studied extensively and plausible models have been proposed. However, it is still debated whether trapping of PARP1/2 on chromatin reflects exclusively the suppression of its catalytic activity, or whether a PARP-inhibitor-dependent reverse allosteric process independently enhances chromatin binding and largely determines inhibitor efficacy – possibly with contributions from proteins completing the PARP catalytic site, such as HPF1 [7,8,10–18]. In addition to classical BRCA1/2 mutations, deficiencies in HR repair genes such as PALB2, RAD51 and its paralogs, as well as several others, show synthetically lethal interactions with PARPis and extend the spectrum of tumors that may be targeted with these compounds [19–21].

Despite striking successes, this approach has limitations, as HR-deficient tumors represent a small percentage of all human tumors, and of these only 30——50 % respond to PARPi monotherapy [22] – owing primarily to de novo resistance to the inhibitor, or resistance acquired by HR restoration, or the acquisition of compensatory mutations [23,24]. As one strategy to overcome these limitations and improve therapeutic efficacy, combinations of PARPis with radiotherapy (RT) have been explored. Indeed, olaparib radiosensitizes lung and pancreatic cancer cells in vitro and in vivo, but only in an HR-deficient background, or after combined treatment with ATR inhibitors [25,26].

Recent studies highlight the PARPi, talazoparib, as a highly potent radiosensitizer in a broad range of HR-proficient cancer cell lines, effective at low nanomolar concentrations (2——250 nM), and even after short exposure times (~1h) [27,28]. Notably, the radiosensitizing efficacy of talazoparib is superior to that of other PARPis, such as PJ34 and even olaparib, veliparib, or rucaparib [27–32], making it a highly promising compound for clinical application. Since talazoparib radiosensitization varies among tumor cells [27,31], it is important to develop means to predict and possibly further enhance its radiosensitizing properties. It has been proposed that radiosensitizers in general and talazoparib in particular increase the sensitivity of cells to IR by shifting the balance of DSB processing from error-free to error-prone repair pathways [27,28,33,34].

The mechanistic foundations of this response are as follows: Two main pathways repair DSBs in mammalian cells: classical non-homologous end joining (c-NHEJ) and homologous recombination repair (HR). c-NHEJ rejoins DSBs with fast kinetics, accepting sequence errors at the junction or the joining of wrong ends [35]. HR, on the other hand, utilizes the sister chromatid available in the S- (partly) and G_2 phases of the cell cycle and repairs DSBs in an error-free manner [35–39]. Cells also utilize a set of mechanistically distinct repair pathways, collectively called alternative end joining (alt-EJ), which in addition to some first-line normal engagement, also backup c-NHEJ or HR processing failures [36,40–43]. Compared to HR, and even c-NHEJ, alt-EJ is more error-prone, causing large deletions and often joining unrelated DSB ends to form chromosomal translocations. However, overall and as expected from its evolutionary history, alt-EJ helps to maintain genomic integrity [36,40,44]. In this context of processing options, our work with talazoparib shows that radiosensitization can be attributed to a shift from c-NHEJ, and to a lesser degree from HR, to alt-EJ [27,28]. Indeed, talazoparib treatment promotes the recruitment of RPA to DSB sites and antagonizes the c-NHEJ promotor 53BP1, while exerting inhibition of c-NHEJ in pulsed-field gel electrophoresis experiments equivalent to that of DNA-PKcs inhibition [27,28]. Collectively, these results document a shunting of DSBs from c-NHEJ to alt-EJ.

Alt-EJ pathways benefit from short-range resection initiated by the CtIP/MRN (MRE11, Rad50, and NBS1) complex [40,45–47]. One sub-pathway of alt-EJ utilizes PARP1 and is inhibited in cells treated with talazoparib [42,48]. A second and probably mechanistically distinct sub-pathway of alt-EJ utilizes DNA polymerase theta (Polθ, encoded by the POLQ gene) [44,49,50]. Polθ is a multi-domain protein with a helicase-like domain, a large central domain and a C-terminal polymerase domain. The helicase-like domain of Polθ facilitates annealing of the 3′ overhang pair and scans for short stretches of microhomologous sequence, while the polymerase domain performs fill-in synthesis of missing DNA segments during DSB processing [51,52]. In addition to its well-defined role in IR-induced DSB repair, Polθ has also been reported to be involved in sealing ssDNA gaps during replication [53], as well as facilitating translesion synthesis during the repair of high LET-induced, complex DSBs [54]. These inherently error-prone DNA repair mechanisms can lead to templated nucleotide insertions and microhomology-flanked deletions, and can also cause chromosomal rearrangements [51,52].

A recent study shows that Polθ-mediated end-joining takes over DSB repair when c-NHEJ becomes suppressed [55]. This suggests that Polθ-mediated alt-EJ is active in talazoparib-treated cells, where c-NHEJ-inhibition is considered a key component of the induced radiosensitization [27]. This notion is further supported by the fact that IR-induced chromosomal translocations, a hallmark of suppressed c-NHEJ activity, are significantly increased after exposure to talazoparib [27,28]. We therefore hypothesized that inhibition of Polθ-mediated alt-EJ would further radiosensitize talazoparib-treated cells.

Tumors with POLQ defects are rare in cancer patients. On the contrary, POLQ is often overexpressed in HR-deficient tumors – and occasionally in cancers with functional HR [49,56–58]. Therefore, the development of Polθ inhibitors to specifically target susceptible cancers through synthetic lethal interactions is being intensively pursued. As part of these efforts, the widely used antibiotic, novobiocin (NVB), was uncovered as a promising Polθ inhibitor, and Artios reported ART558 and several other related compounds as highly specific Polθ inhibitors. Both compounds are presently tested in preclinical and clinical settings; they show promising results as single agents in tumors with appropriate genetic backgrounds – notably deficiencies of BRCA1/2, RAD54, and 53BP1 [58–61]. These inhibitors are useful tools to investigate how Polθ inhibition may affect talazoparib radiosensitization.

Here, we report that genetic ablation or chemical inhibition of Polθ in cancer cells often induces only modest radiosensitization, whereas it markedly radiosensitizes talazoparib-treated cells. Mechanistically, by inhibiting c-NHEJ and PARP1-dependent alt-EJ and enhancing DNA end resection, talazoparib creates favorable conditions for the engagement of Polθ-mediated alt-EJ that is suppressed by its inhibitors resulting in enhanced radiosenstization.

Methods and materials

Cell lines

A549 parental and POLQm (POLQ exon1 knockout) cells [62]; U2OS parental, U2OS POLQm (POLQ exon16 mutant) [63] and U2OS DR-GFP and EJ-2 cell lines (a gift from Dr. J. Stark) [64]; RPE-1 and 82–6 hTert cells were cultured at 37 °C in a 5 % CO_2, 95 % air atmosphere. Details on procedures, conditions, and reagents are provided in "Supplementary Methods and Materials".

Inhibitors and antibodies

Details are provided under Supplementary Methods and Materials.

Radiation exposure

Irradiations were carried out with an X-ray machine (GE Healthcare) operated at 320 kV, 10 mA with a 1.65 mm Al filter (effective photon energy approximately 90 kV). The dose rate at 50 cm was approximately 2.8 Gy/min.

Clonogenic survival assay

Exponentially growing cells were treated with the indicated

inhibitors for 1 h before IR. At 6 h post-IR, cells were plated for colony formation in the absence of drugs. Cells were allowed to grow colonies for 8–12 days. Colonies were fixed and stained with crystal violet (see "Supplementary Methods and Materials" for details).

Indirect immunofluorescence (IF) and image analysis

Cells grown on coverslips were labeled with 10 μM of 5-ethynyl-2′-deoxyuridin (EdU) for 30 min before treatment with the indicated inhibitors. After treatment, cells were exposed to IR. Inhibitors were maintained throughout the experiment. Cells were fixed in PFA solution (3 % paraformaldehyde and 2 % sucrose), permeabilized in 0.5 % Triton-X100 in PBS, and blocked in PBG solution (0.2 % fish skin gelatin, 0.5 % BSA fraction V, in PBS). Cells were then stained for RPA70 or γ-H2AX; cell nuclei were stained with DAPI (see "Supplementary Methods and Materials" for details).

Samples were scanned on an AxioScan.Z1 imaging platform (Zeiss) for high-throughput analysis by quantitative image-based cytometry (QIBC). Image analysis was carried out as described elsewhere [65]. For cell cycle-specific analysis of DSB repair, foci were scored in EdU^- and EdU^+cells as indicated; data obtained were processed using the Imaris software and organized using the software, Orange.

Pulsed-field gel electrophoresis (PFGE)

PFGE was used to assess the induction and repair of DSBs as described elsewhere [66]. Details are given under "Supplementary Methods and Materials".

Cytogenetic analysis

Exponentially growing cells were treated with the indicated inhibitors for 1 h prior to IR exposure and allowed to repair for 1–5 h at 37 °C. 0.1 mg/mL Colcemid (Biochrom AG) was added to each sample during the last 1 h to accumulate metaphases, as described elsewhere [67]. Approximately 100 metaphases were analyzed for chromosomal abnormalities. Analysis was performed using bright field microscopy (Leica Microsystems DM RBE, Wetzlar, Germany).

RNA interference and immunoblotting

Transfection with specific siRNAs was performed using the Nucleofector device (Amaxa Biosystems). Details of siRNAs are provided in "Supplementary Methods and Materials". The level of knockdown was analyzed by Western blotting. Protein extracts were prepared and run on SDS-PAGE gels using standard protocols, as described previously [39]. Imaging was performed with the Odyssey scanner (LI-COR).

Statistical analysis

Graphs were generated in SigmaPlot 14. Statistical significance was determined using the Student's *t*-test function in SigmaPlot 14.

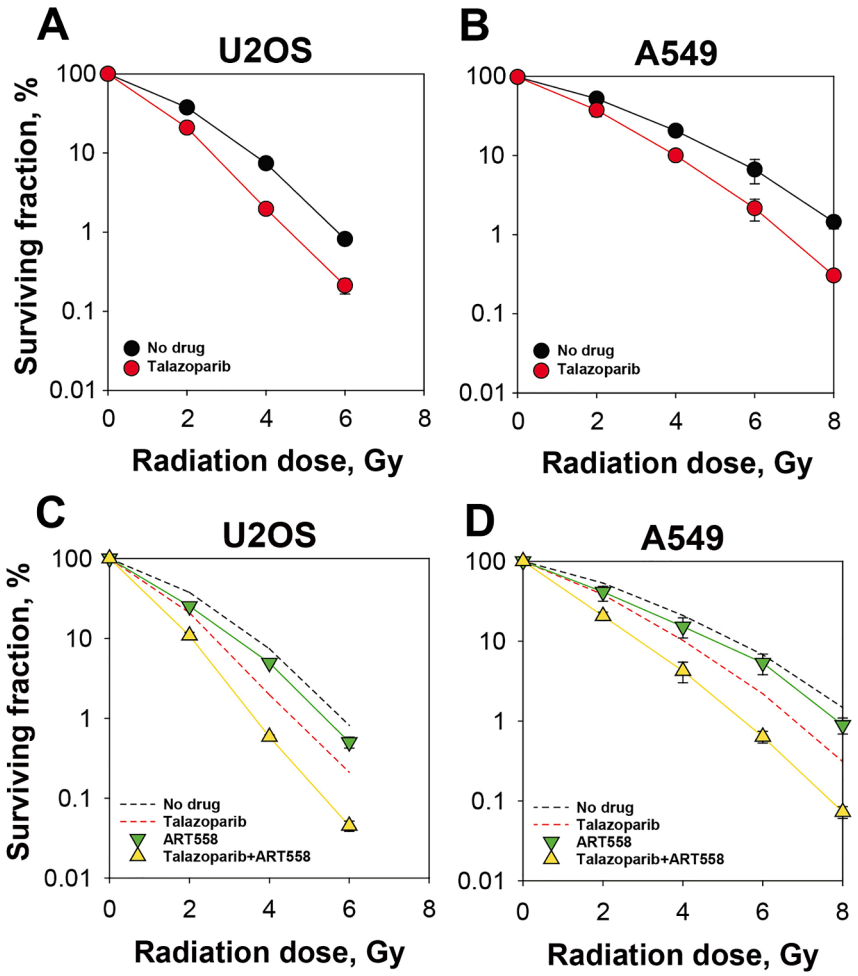

Fig. 1. *Talazoparib radiosensitization is enhanced by suppression of Polθ activity.* (A) Clonogenic survival in U2OS cells showing radiosensitization after 6 h incubation with 50 nM talazoparib; (B) Radiosensitization assessed as in (A) for A549 cells; (C) Radiosensitization by a combination of 50 nM talazoparib and 5 μM ART558 in U2OS cells; (D) Radiosensitization assessed as in (C) for A549 cells. Data represent mean ± SD calculated from three independent experiments.

Statistical significance is indicated as * $p < 0.05$, ** $p < 0.01$, or *** $p < 0.001$.

Results

We focused our experiments on the osteosarcoma U2OS and the lung carcinoma A549 cell lines, since available POLQ mutants offer a platform to test our hypotheses. Fig. 1A and 1B show that talazoparib applied at 50 nmol/L for 6 h, effectively radiosensitizes both cell lines. Notably, while the Polθ inhibitor ART558 only marginally radiosensitizes these cells, it induces strong, further radiosensitization in talazoparib-treated cells (Fig. 1C and 1D). Similar results are obtained with a second Polθ inhibitor, novobiocin (NVB) (Figure S1A and B). To further test the validity of the above observations, we analyzed mutants genetically deficient in POLQ. Genetic ablation of POLQ in U2OS or A549 cells causes a small degree of radiosensitization (Fig. 2A and Figure S2A). However, when these mutants are treated with talazoparib, the Polθ defect results in pronounced radiosensitization (Fig. 2A and Figure S2A). The radiosensitizing effect of the POLQ knockout is stronger than that of the tested inhibitors, suggesting that under the inhibitor concentrations and treatment times employed, Polθ inhibition is incomplete.

We next investigated how POLQ deficiency affects radiosensitivity of cells exposed to olaparib, veliparib or rucaparib, PARPis with weaker radiosensitizing potential than talazoparib [27,31,32]. The results confirm the stronger radiosensitizing potential of talazoparib and show that suppression of Polθ activity fails to generate additional radiosensitization (Fig. 2B, 2C, 2D and Fig. Figure S2B, C, D). We reported that talazoparib fails to radiosensitize normal cell lines [27]. Here, we investigated whether this specificity persists when talazoparib is combined with Polθ inhibitors. The results with the non-transformed human cell lines, RPE-1 and 82-6hTert, in Figure S3A, B show that indeed talazoparib fails to radiosensitize normal cells even when combined with Polθ inhibitors.

We conclude that treatment of cancer, but not normal, cells with talazoparib renders them more susceptible to subsequent Polθ inhibition. We hypothesized that talazoparib somehow increased utilization of Polθ-dependent alt-EJ, which was suppressed when the inhibitor was administered causing thus the increased radiosensitization. In the following section we describe experiments that helped to elucidate the mechanism of talazoparib radiosensitization in cancer cells and its ability to synergize with Polθ ablation.

We postulated that if treatment with talazoparib, inhibits c-NHEJ and enhances utilization of Polθ-mediated alt-EJ [27], talazoparib-treated cells genetically deficient in POLQ or treated with Polθ-inhibitors, should display altered DSB repair kinetics, as typically alt-EJ operates with slow kinetics. To investigate this, we analyzed the formation and decay of γ-H2AX foci, an accepted proxy for DSBs, in the genomes in U2OS and A549 cells. Fig. 3A and 3B show that the kinetics of γ-H2AX foci induction and decay (2 Gy) are indistinguishable in POLQ mutant (POLQm)-U2OS cells and the corresponding POLQ proficient control. In contrast, in talazoparib-treated POLQm cells, markedly delayed kinetics are observed as compared to talazoparib-treated POLQ proficient cells. A similar, albeit less pronounced inhibition is observed

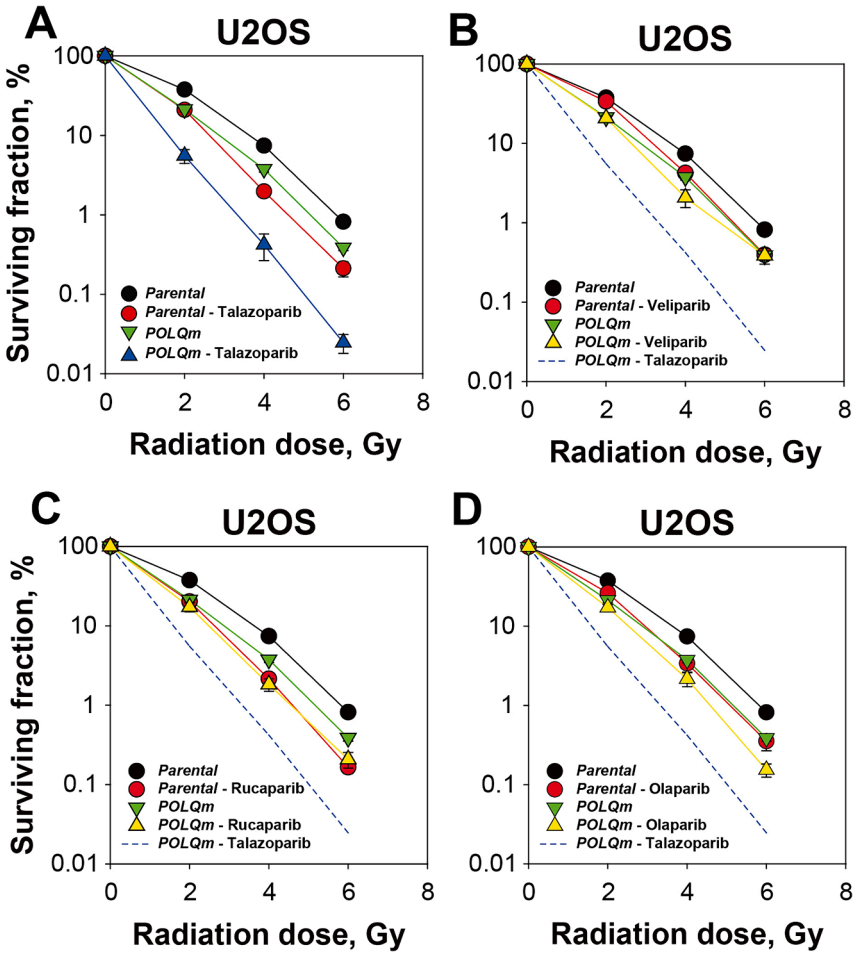

Fig. 2. *Comparison of talazoparib radiosensitization with that of other PARP inhibitors in POLQ deficient cells.* Clonogenic survival assays quantitating effects of (A) 50 nM talazoparib, (B) 5 μM veliparib, (C) 5 μM rucaparib, and (D) 3 μM olaparib in U2OS parental and POLQm cells. Data represents mean ± SD calculated from three independent experiments.

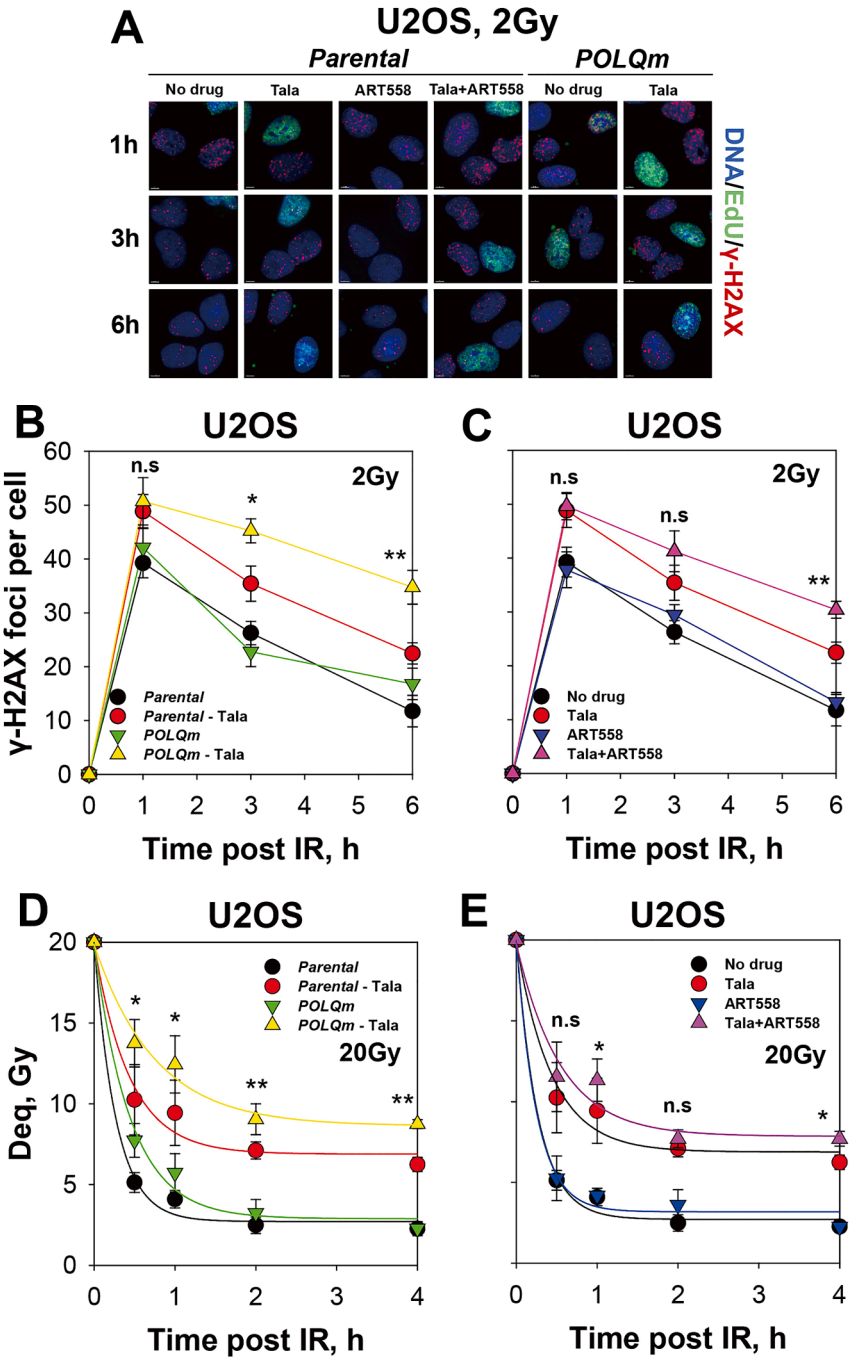

Fig. 3. *Talazoparib combined with Polθ inhibition suppresses IR induced DSB repair.* (A) Representative images of γ-H2AX foci in U2OS cells. Scale bar: 5 μm; (B) Effects of 50 nM talazoparib on γ-H2AX foci kinetics in exponentially growing U2OS parental and POLQm cells; (C) Effects of 50 nM talazoparib and/or 5 μM ART558 on γ-H2AX foci kinetics in exponentially growing U2OS cells; (D) Effects of talazoparib on DSB repair kinetics in U2OS parental and POLQm cells exposed to 20 Gy and analyzed by PFGE; (E) as in (D) for combined talazoparib and/or ART558 treatment. Data represent mean ± SD calculated from two to three independent experiments. Statistical analysis is performed between talazoparib- and talazoparib + Polθ inhibition treated groups, * $p < 0.05$, ** $p < 0.01$, *** $p < 0.001$. n.s, nonsignificant.

using the ART558 inhibitor (Fig. 3C), as well as in A549 cells after genetic inactivation of POLQ, or inhibition of Polθ (Figure S4A, B and C). The Polθ-independent increase at 1 h of γ-H2AX foci following treatment with talazoparib, reflects the above discussed shift in repair pathway engagement that generates a higher net of unrepaired DSBs.

As an extension of the above analysis, we measured under similar conditions induction and repair of DSBs using PFGE. PFGE detects DNA ruptures directly by applying the physical principles of gel electrophoresis, rather than the indirect DDR signaling-marking of γ-H2AX that obeys, when carefully analyzed, the delayed kinetics of induction and decay of the DDR rather than the physical induction and repair of DSBs [66]. However, the sensitivity of PFGE requires high IR doses, and we have reported dramatic shifts in the engagement of HR versus c-NHEJ with increasing IR dose [39]. Indeed, while engagement of HR can reach 50 % at doses much below 2 Gy, it hovers around 10–20 % between 2–5 Gy, and is practically undetectable above 10 Gy [39].

PFGE experiments, typically require doses between 10–20 Gy and detect therefore mainly c-NHEJ and alt-EJ. Under these conditions,

talazoparib strongly inhibits c-NHEJ, as previously reported [27]. On the other hand, Polθ genetic defects leave unchanged DSB repair in U2OS cells, but clearly inhibit repair in talazoparib-treated cells (Fig. 3D). The response is similar in U2OS cells treated with ART558, although the effect is smaller failing to reach statistical significance – again possibly owing to the inhibitor concentrations employed (Fig. 3E). The results with A549 cells also show similar overall trends, although for similar reasons, the effects are small and fail to reach statistical significance (Figure S4D, E).

Thus, talazoparib inhibits c-NHEJ and as a consequence, it increases the number of γ-H2AX foci detected at 1 h and the fraction of DSBs processed with slow kinetics by alt-EJ, as we had postulated (Table S1). The latter effect is markedly increased upon suppression of Polθ activity, signifying a larger functional contribution of the protein in talazoparib-treated cells as compared to untreated controls, where its inhibition has no detectable effect. Since talazoparib inhibits PARP1, PARP1-

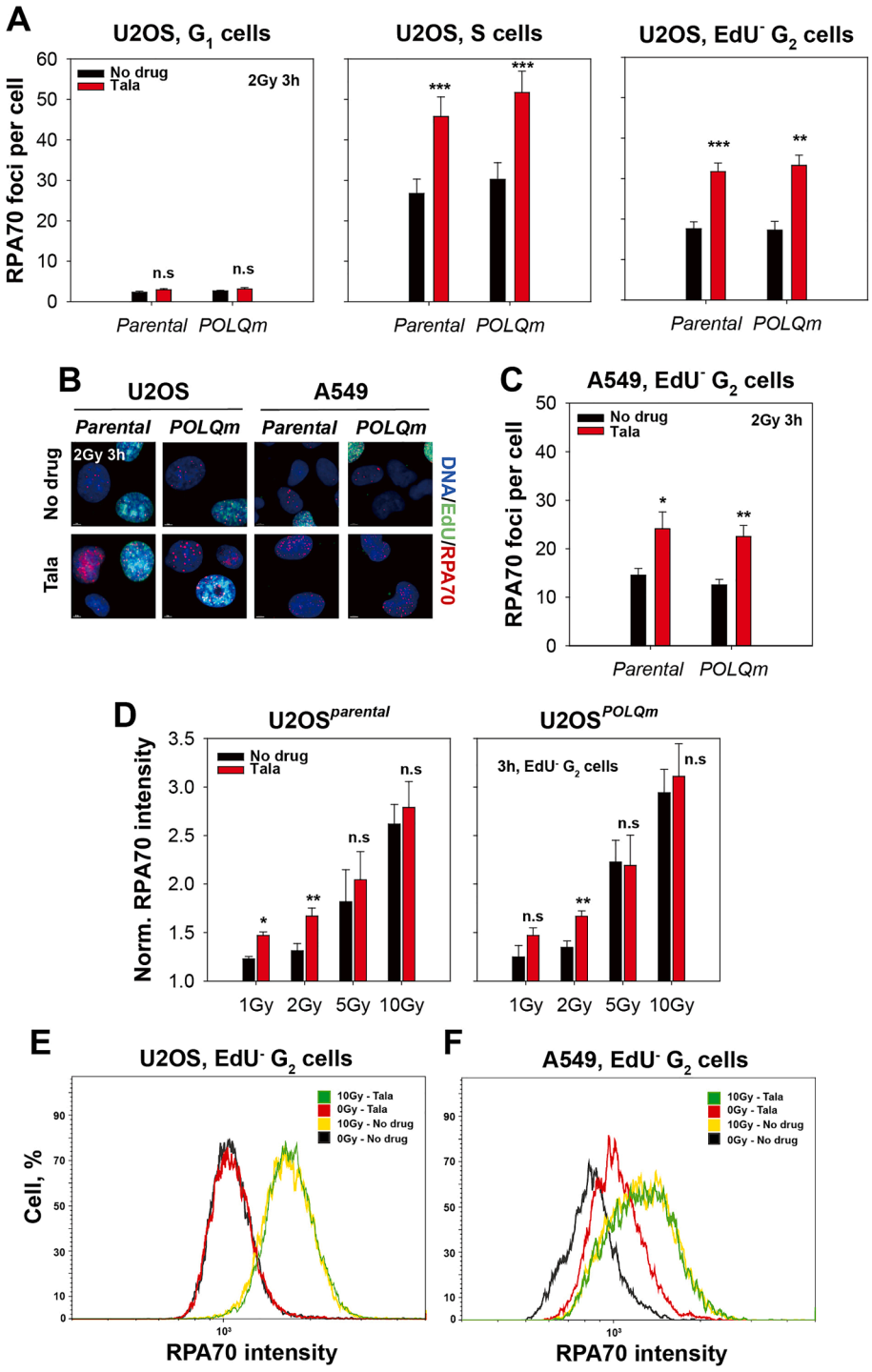

Fig. 4. *DSB end resection in cells treated with talazoparib.* (A) Quantification of IR induced RPA70 foci in U2OS parental and POLQm cells after treatment with/without 50 nM talazoparib throughout the cell cycle; (B) Representative IF images of RPA70 foci in U2OS and A549 cells. Scale bar: 5 μm; (C) As in (A) for EdU$^-$ G_2 −A549 cells; (D) As in (A) for EdU$^-$ G_2 −U2OS parental and POLQm cells exposed to low and high IR doses; (E) FC-based analysis of resection in U2OS cells. Resection is measured 3 h after exposure to 10 Gy and treatment with/without 50 nM talazoparib; (F) As in (E) for A549 cells. Data represent mean ± SD calculated from three independent experiments (except Figure D, n = 2). * $p < 0.05$, ** $p < 0.01$, *** $p < 0.001$. n.s, nonsignificant.

dependent alt-EJ is suppressed, leaving Polθ dependent alt-EJ to function. In the following experiments we show how talazoparib generates conditions that increase the engagement at DSBs of Polθ-dependent alt-EJ and other resection dependent DSB repair pathways [65].

Because alt-EJ benefits from resection and CHO cells that are effectively radiosensitized by talazoparib also show increased resection [27], we introduced QIBC and flow cytometry to carry out cell cycle specific resection analysis, at low and high IR doses respectively, by scoring RPA foci in U2OS and A549 cells (Figure S5); see also [38,65,68]. Fig. 4A and B show active resection at DSBs in U2OS cells 3 h after exposure to 2 Gy in S- and the G_2- phases of the cell cycle. Resection is practically undetectable in G_1-phase. Notably, treatment with talazoparib markedly increases resection in the S- and G_2-phase paving thus the way to a redirect DSBs to Polθ alt-EJ. Similar responses are observed in POLQ-deficient A549 cells (Fig. 4B and 4C). Notably, talazoparib fails to increase resection at high IR doses as measured either by QIBC (Fig. 4D), or FACS (Fig. 4E, 4F), suggesting regulatory mechanisms that suppress its function with increasing IR dose [27] (see above for a discussion of similar responses regarding HR engagement).

To elucidate how resection contributes to the effects of talazoparib and particularly to the increased radiosensitization by Polθ inhibition of talazoparib-treated cells, we employed RNAi to suppress resection. CtIP is a crucial regulator of resection [69] and its knockdown (Fig. 5A) dramatically reduces resection in both U2OS parental and POLQm cells (Fig. 5B and C). Notably, despite radiosensitization of CtIP depleted cells, talazoparib radiosensitization is similar in CtIP depleted and untreated cells (Fig. 5D – compare shaded areas). We conclude that talazoparib radiosensitization also has a resection-independent component.

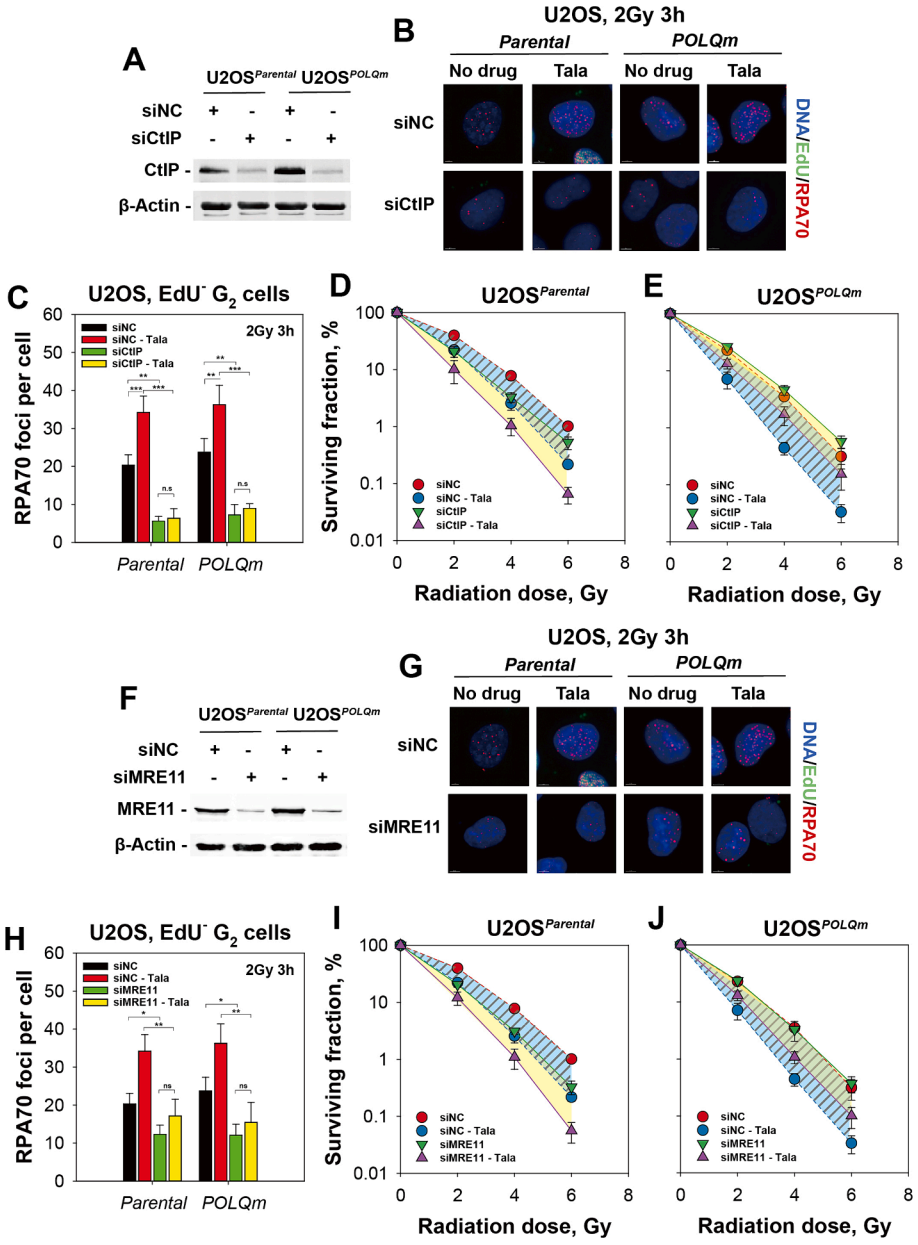

Fig. 5. *CtIP and MRE11 mediated DSB end resection after treatment with talazoparib contributes to radiosensitization by Polθ activity suppression.* (A) Western blot depicting knockdown of CtIP in U2OS cells; (B) Representative IF images of RPA70 foci in U2OS cells. Scale bar: 5 μm; (C) Quantification of IR induced RPA70 foci after CtIP depletion in U2OS parental and POLQm cells after treatment with/without 50 nM talazoparib; (D) Impact of CtIP depletion on the radiosensitizing effect of 50 nM talazoparib in U2OS cells; (E) same as in D for POLQm U2OS cells; (F, G, H, I, J) as in (A, B, C, D, E, respectively) following MRE11 depletion. Shading serves to subjectively guide an estimation of the radiosensitizing effect of talazoparib on control and knockdown cells, respectively. Data represent mean ± SD calculated from three independent experiments. * $p < 0.05$, ** $p < 0.01$, *** $p < 0.001$. n.s, nonsignificant.

In POLQ deficient cells (Fig. 5E – compare shaded areas), on the other hand, we detect reduced radiosensitization after CtIP depletion, and the increased radiosensitization by talazoparib is partly lost. The observation that in POLQm cells CtIP depletion exerts lesser radiosensitization, suggests that the associated resection benefits Polθ mediated repair.

Since CtIP closely cooperates with the MRN complex, we also assessed the impact of MRE11 depletion, the subunit of MRN responsible for nuclease activity [70,71]. Fig. 5F shows efficient knockdown of MRE11 in U2OS cells, while Fig. 5G and 5H demonstrate that this depletion causes marked reduction in resection, albeit weaker than CtIP. The effects of MRE11 depletion on cell radiosensitization (Fig. 5I, J) parallel well those of CtIP depletion, but are again less pronounced. Overall, the above results are also validated in A549 cells (Figure S6B, C, E, F).

Since HR may also benefit from talazoparib induced increased DSB end resection, we analyzed RAD51 foci formation in talazoparib treated cells. Figure S7A shows a small increase in RAD51 foci in parental U2OS cells exposed to talazoparib and analyzed in the G_2-phase. In POLQ deficient U2OS cells, RAD51 foci numbers increase, as reported previously [49], and treatment with talazoparib fails to generate further increases (Figure S7B). Despite elevated resection and increased RAD51 foci formation in talazoparib-treated cells, HR activity measured by the DR-GFP reporter assay remains unchanged (Figure S7C). Collectively, we surmise that HR is only mildly affected by talazoparib in the tested

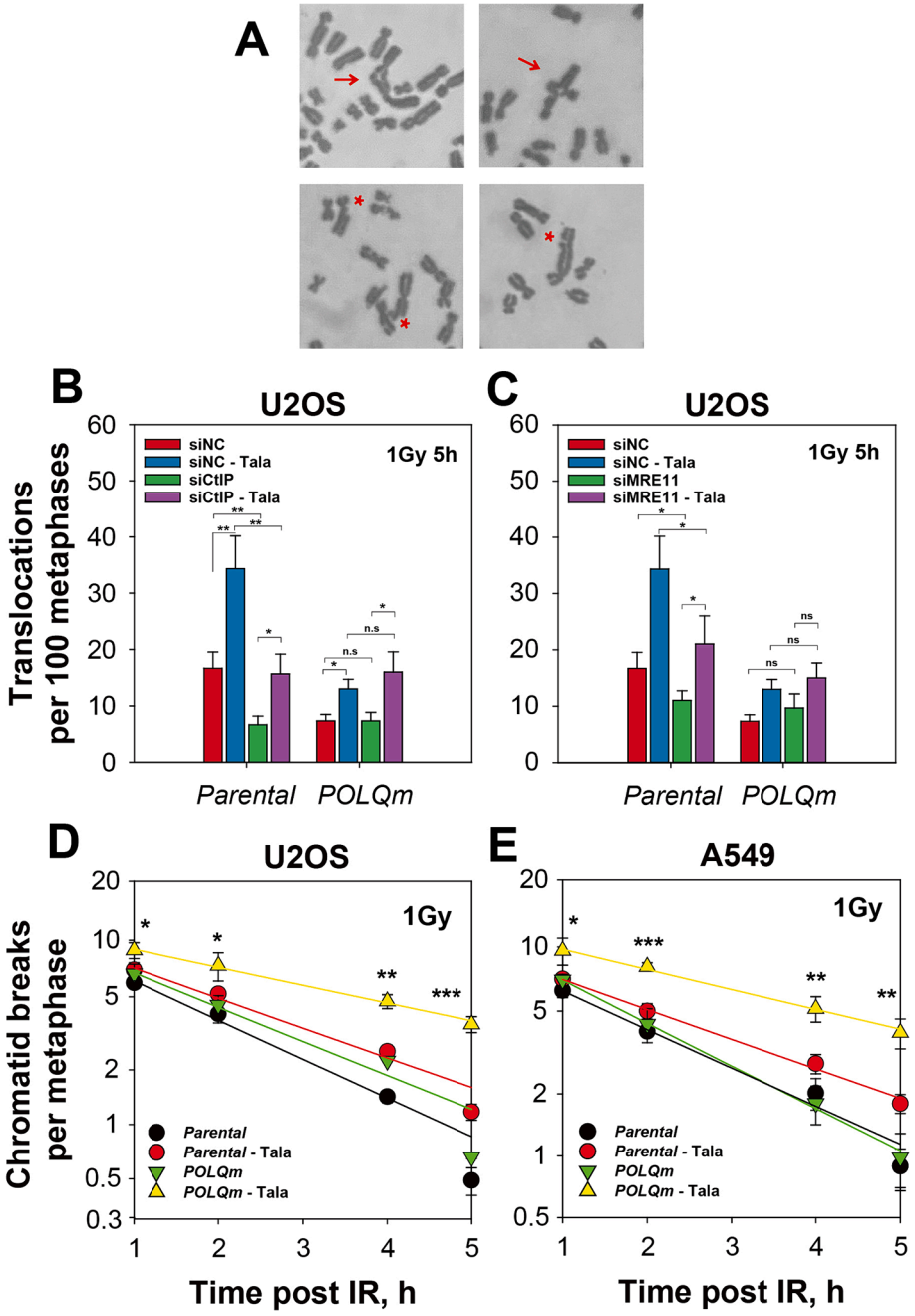

Fig. 6. *Polθ inhibition suppresses talazoparib-induced translocations and increases chromatid breaks.* (A) Representative images of chromatid translocations (indicated by arrow) and breaks (indicated by asterisk); (B) Frequency of IR induced translocations in CtIP depleted U2OS parental and POLQm cells after treatment with/without 50 nM talazoparib; (C) As in (B) after MRE11 depletion; (D) Effects of 50 nM talazoparib on IR-induced chromatid-break-repair in U2OS parental and POLQm cells; (E) As in (D) for A549 parental and POLQm cells. Data represent mean ± SD calculated from three independent experiments. Statistical analysis is performed between talazoparib- and talazoparib + Polθ inhibition treated groups, * $p < 0.05$, ** $p < 0.01$, *** $p < 0.001$. n.s, nonsignificant.

cell lines and that the associated radiosensitization derives predominantly from effects in other DSB repair pathways –mainly c-NHEJ. The EJ2-GFP reporter cell system (Figure S7D), designed to detect alt-EJ activity, confirms contributions from Polθ, and shows that actually talazoparib, but not olaparib, leaves alt-EJ unaffected; yet combined with ART558 talazoparib produces robust alt-EJ inhibition.

Since alt-EJ and resection are linked to the formation of chromosome translocations, we analyzed chromosomal abnormalities at metaphase, as the next step in our analysis of the effects of Polθ defects on talazoparib treated cells. We analyzed translocations and breaks in U2OS and A549 cells exposed to 1 Gy in G2-phase [67], by collecting metaphases 5 h post irradiation. Fig. 6A, B, C, and Figure S8A show that talazoparib causes a 2-fold increase in translocation formation, an effect likely moderated somewhat by the inhibition of PARP1 in talazoparib treated cells [42]. Suppression of resection by CtIP depletion reduces translocations by over 50 % both in control and talazoparib treated cells. However, as with cell survival, a resection independent component is detected in translocation formation as well, in talazoparib treated cells (Fig. 6B). These results support the postulated activation of error-prone DSB processing in talazoparib treated cells that is only partly resection dependent.

POLQ genetic deficiency or protein inhibition with ART558 suppresses translocation formation in control, and more strongly in talazoparib treated cells. However, under conditions of suppressed resection, the response following Polθ inhibition is normalized and translocations form at similar levels in POLQm and parental cells (Fig. 6B, C and Figure S8A, B). Similar trends are also observed in U2OS cells after depletion of MRE11 (Fig. 6C).

We also analyzed the kinetics of chromatid break repair by collecting metaphases using a 1 h colcemid window applied at different times after exposure of cells to 1 Gy for up to 5 h. Fig. 6D summarizes the results obtained with U2OS cells. Untreated parental cells repair chromatid breaks with a half time of ~ 2h (Table S2). Treatment with talazoparib only slightly increases this time. This is not surprising as we have reported that chromatid break repair mainly reflects the function of HR [67], which remains largely unaffected by talazoparib (see above). Also, POLQ-deficient U2OS cells repair chromatid breaks with similar efficiency. Strikingly, when POLQ mutant cells are exposed to talazoparib, a strong, statistically significant reduction in chromatid break repair is observed. We suggest that this reflects suppression in the rejoining of the subset of DSBs normally engaging in translocation formation, which now remain as chromatid breaks and are processed, in addition to HR by slower functioning Polθ independent alt-EJ pathways. Similar results are obtained using ART558 in parental cells (Figure S8C), as well as in A549 cells (Fig. 6E and Figure S8D). Table S2 summarizes the kinetics analysis of these experiments.

Discussion

PARPis are used in the clinic as chemotherapeutic agents to treat BRCA1/2 deficient tumors and function through synthetic lethal interactions with HR defects [1–6]. However, the development of resistance, normal tissue toxicity, and the limited therapeutic spectrum owing to their dependence on HR-defects limit their application. Therefore, the importance of exploring combinations with other treatment modalities, like RT, to widen their application spectrum in the management of cancer, is widely recognized. Recent mechanistic studies show that talazoparib is a potent and unique radiosensitizer, effective even at low drug doses [27,28] paving thus the way for combinations with RT.

Highly relevant clinical work tested talazoparib as a single agent in the treatment of cancer and recent toxicity data are promising, but suggest that high doses should be avoided [72–74]. A prospective phase II study also showed efficacy in patients with HR defects [75] and the TALASUR trial generated promising results in combination with immune checkpoint inhibitors [76]. The first analysis of a randomized, placebo-controlled, phase-3 trial, TALAPRO-2, including 805 patients with metastatic castration-resistant prostate cancer showed better radiographic, progression-free survival rates in the talazoparib combination treatment arm versus standard of care [77]. Nevertheless, clinical trials combining talazoparib with radiotherapy are scarce, despite the striking properties of the compound as a cell radiosensitizer [27–32].

Existing data show that talazoparib radiosensitization varies depending on the cell line tested and is at times limited [27,31,32]. Therefore, we sought means in the present work to further increase this effect in an effort to generate tools that may improve and accelerate its clinical application. Prompted by the observation that talazoparib radiosensitization involves the shunting of DSBs to alt-EJ, and because talazoparib inhibits PARP1 and PARP2, and thus PARP-dependent alt-EJ, we explored inhibition of Polθ as a strategy to suppress Polθ dependent alt-EJ. Since several tumors overexpress Polθ [49,56,57], combining Polθ inhibitors with talazoparib and RT offers means to improve the therapeutic window of the compound and extend it even to PARPi resistant cancers.

Radiosensitization has been observed by both genetic ablation and chemical inhibition of Polθ in HR proficient cells. Higgins' group demonstrated that knockdown of POLQ significantly increased the sensitivity of SQ-20B and HeLa cells to IR [78]. Similarly, ART558 effectively radiosensitized HCT116 and H460 cells. Notably and significantly for radiotherapy, the radiosensitizing effect was further enhanced when radiation was administered in daily fractions [79]. Rao et al. [80] also reported that NVB treatment enhanced radiosensitivity in A549 and H460 cells, albeit to a lesser extent than ART558.

The present study confirms these findings, although lower levels of radiosensitization were detected by POLQ ablation or ART558 treatment; and NVB failed to radiosensitize. There are multiple reasons for these differences including the short duration of drug exposure in our study (6 h), compared to 24 h by Rao et al. [80] and 72 h by Rodriguez-Berriguete et al [79]. Differences in plating protocols to assess cell survival add to the possible causes, as we treated unperturbed, exponentially growing cultures that we plated afterward, while freshly trypsinized pre-plated cells at widely different numbers, were treated by others [79]. Finally, in agreement with our results, lack of radiosensitization in normal cells exposed to Polθ inhibitors was previously reported by Higgins et al. [78]. Thus, the radiosensitizing effect of Polθ inhibition is well-documented and the moderate, cell specific effects observed hint to opportunities for improvements. The present study is a step in this direction.

Our DSB repair pathway-specific analysis of the talazoparib effects identified c-NHEJ as a key target. This notion is also supported by a report [81] showing that PARP1 inhibition by talazoparib is associated with loss of Ku80, 53BP1 and RIF1 from DSB sites, resulting in over-resected DSBs. We also showed that following c-NHEJ abrogation, free DSB ends are subjected to resection that in-turn increased engagement of Polθ alt-EJ. This increased engagement of Polθ alt-EJ automatically generated an opportunity for increased radiosensitization by Polθ activity suppression.

Polθ restricts RAD51 recruitment to and dissociates RPA from resected DSBs, facilitating alt-EJ at the expense of HR repair [33,34]. We show here that similar trends are detectable after treatment with talazoparib that compromises c-NHEJ. Indeed, we proposed some time ago that alt-EJ (possibly all subpathways) is the ultimate backup for abrogated c-NHEJ and HR [40]. In line with the importance of increased resection in talazoparib-treated cells for increased engagement of Polθ alt-EJ, we showed that suppressing resection by depleting CtIP or MRE11 [40,45–47] impaired the effectiveness of Polθ inhibition. Also, recent evidence suggests that the level of DSB resection is an important efficacy determinant of Polθ inhibitors. Thus, Patterson-Fortin et al. [82] demonstrated that the synthetic lethality between NVB and a DNA-PKcs inhibitor is substantially compromised when resection is suppressed by EXO1/BLM knockdown. Also, Krais et al. [83] reported that compared to BRCA1 null cells, PALB2 and BRCA2 mutant cells that retain resection

activity show higher dependency on Polθ for viability.

Finally, we demonstrated that Polθ mediated alt-EJ is partly responsible for the formation of IR-induced translocations in talazoparib-treated cells. It is noteworthy, however, that Polθ inhibition fails to abolish talazoparib-induced translocations completely, which hints to other error-prone repair pathways, possibly also relying on resection, but also to resection-independent pathways. Notably, talazoparib retains radiosensitizing potential under conditions of suppressed resection following CtIP or MRE11 knockdown. Our results on chromosomal translocation formation and alt-EJ measured by EJ2 reporter assay suggest that inhibition of Polθ adds to the alt-EJ inhibition effect of PARP1 inhibition by talazoparib [42]. This is in line with independent branches of alt-EJ inhibition. It has been shown that combined deficiency of Polθ and PARP1 generated additive effects on the viability of BRCA-deficient cells, again suggesting that PARP1-mediated and Polθ-mediated alt-EJ may function independently [59–61]. Yu et al. [50] also demonstrated that DSBs induced in G1 can be repaired by alt-EJ during S-G2/M phases in a Polθ-dependent, but PARP1-independent manner. Therefore, it seems reasonable to assume that sub-pathways of alt-EJ exist that utilize existing components in a context-dependent manner.

In aggregate, our findings inform a novel strategy for treating a broad spectrum of tumors irrespective of their HRness. Such a combination may work at significantly lower drug concentrations, as well as radiation doses, which would certainly help in reducing therapy side effects.

Conclusion

We report a novel radiosensitizing strategy for cancer cells using a combination of talazoparib and Polθ inhibitors. The mechanisms underpinning increased radiosensitization reflect an enhanced utilization of alt-EJ in talazoparib-treated cells that is suppressed by the inhibition of Polθ activity. The findings may be translated into an effective treatment strategy applicable in a broad spectrum of cancers, independently of their HR-profile. Towards this goal predictors of talazoparib radiosensitization and Polθ activity in talazoparib treated cells need to be developed. The combination proposed here may also be useful in overcoming PARPi resistance.

Conflicts of interest

Martin Stuschke: AstraZeneca (Advisory Board Function, Research and Clinical Trials), Bristol-Myers Squibb (Advisory Board Function), Sanofi-Aventis (Advisory Board Function) and Janssen-Cilag (Advisory Board Function). Other authors declare no conflict of interest.

Funding

Research activities in our lab have been funded by grants from BMBF (02NUK037B, 02NUK043B, 02NUK054B) and by the German Research Foundation (DFG-IL51.10, IL51.11, GRK1739) and by the German Federal Ministry for Economic Affairs (BMWi-50WB1836), as well as by DAAD Project #57515880.

CRediT authorship contribution statement

Xixi Lin: Writing – review & editing, Writing – original draft, Visualization, Methodology, Investigation, Formal analysis, Data curation, Conceptualization. **Aashish Soni:** Writing – review & editing, Writing – original draft, Visualization, Validation, Supervision, Methodology, Investigation, Formal analysis, Data curation, Conceptualization. **Razan Hessenow:** Methodology, Formal analysis, Data curation. **Yanjie Sun:** Methodology, Formal analysis, Data curation. **Emil Mladenov:** Methodology, Investigation, Formal analysis, Data curation. **Maja Guberina:** Writing – original draft, Methodology, Formal analysis. **Martin Stuschke:** Supervision, Resources, Project administration, Funding acquisition, Conceptualization. **George Iliakis:** Writing – review & editing, Writing – original draft, Visualization, Validation, Supervision, Software, Resources, Project administration, Funding acquisition, Conceptualization.

Declaration of competing interest

The authors declare that they have no known competing financial interests or personal relationships that could have appeared to influence the work reported in this paper.

Acknowledgments

X. Lin would like to thank the Chinese Scholarship Council (CSC) for the international scholarship support. We acknowledge support by the Open Access Publication Fund of the University of Duisburg-Essen.

Appendix A. Supplementary material

Supplementary data to this article can be found online at https://doi.org/10.1016/j.radonc.2024.110475.

References

[1] Bryant HE, Schultz N, Thomas HD, Parker KM, Flower D, Lopez E, et al. Specific killing of BRCA2-deficient tumours with inhibitors of poly(ADP-ribose) polymerase. Nature 2005;434:913–7.
[2] Fong PC, Boss DS, Yap TA, Tutt A, Wu P, Mergui-Roelvink M, et al. Inhibition of poly(ADP-ribose) polymerase in tumors from BRCA mutation carriers. N Engl J Med 2009;361:123–34.
[3] Konstantinopoulos PA, Ceccaldi R, Shapiro GI, D'Andrea AD. Homologous recombination deficiency: Exploiting the fundamental vulnerability of ovarian cancer. Cancer Discov 2015;5:1137–54.
[4] Farmer H, McCabe N, Lord CJ, Tutt AN, Johnson DA, Richardson TB, et al. Targeting the DNA repair defect in BRCA mutant cells as a therapeutic strategy. Nature 2005;434:917–21.
[5] Pommier Y, O'Connor MJ, de Bono J. Laying a trap to kill cancer cells: PARP inhibitors and their mechanisms of action. Sci Transl Med 2016;8:362ps17.
[6] Helleday T. The underlying mechanism for the PARP and BRCA synthetic lethality: clearing up the misunderstandings. Mol Oncol 2011;5:387–93.
[7] Kedar PS, Stefanick DF, Horton JK, Wilson SH. Increased PARP-1 association with DNA in alkylation damaged, PARP-inhibited mouse fibroblasts. Mol Cancer Res 2012;10:360–8.
[8] Murai J, S-yN H, Das BB, Renaud A, Zhang Y, Doroshow JH, et al. Trapping of PARP1 and PARP2 by clinical PARP inhibitors. Cancer Res 2012;72:5588–99.
[9] Murai J, Huang S-Y-N, Renaud A, Zhang Y, Ji J, Takeda S, et al. Stereospecific PARP trapping by BMN 673 and comparison with olaparib and rucaparib. Mol Cancer Ther 2014;13:433–43.
[10] Petropoulos M, Karamichali A, Rossetti GG, Freudenmann A, Iacovino LG, Dionellis VS, et al. Transcription–replication conflicts underlie sensitivity to PARP inhibitors. Nature 2024;628:433–41.
[11] Langelier M-F, Planck JL, Roy S, Pascal JM. Structural basis for DNA damage-dependent poly(ADP-ribosyl)ation by human PARP-1. Science 2012;336:728–32.
[12] Eustermann S, Wu W-F, Langelier M-F, Yang J-C, Easton Laura E, Riccio Amanda A, et al. Structural basis of detection and signaling of DNA single-strand breaks by human PARP-1. Mol Cell 2015;60:742–54.
[13] Dawicki-McKenna Jennine M, Langelier M-F, DeNizio JE, Riccio Amanda A, Cao Connie D, Karch Kelly R, et al. PARP-1 activation requires local unfolding of an autoinhibitory domain. Mol Cell 2015;60:755–68.
[14] Bilokapic S, Suskiewicz MJ, Ahel I, Halic M. Bridging of DNA breaks activates PARP2-HPF1 to modify chromatin. Nature 2020;585:609–13.
[15] Rudolph J, Jung K, Luger K. Inhibitors of PARP: Number crunching and structure gazing. PNAS 2022;119:e2121979119.
[16] Kanev P-B, Varhoshkova S, Georgieva I, Lukarska M, Kirova D, Danovski G, et al. A unified mechanism for PARP inhibitor-induced PARP1 chromatin retention at DNA damage sites in living cells. Cell Rep 2024;43.
[17] Hopkins TA, Shi Y, Rodriguez LE, Solomon LR, Donawho CK, DiGiammarino EL, et al. Mechanistic dissection of PARP1 trapping and the impact on in vivo tolerability and efficacy of PARP inhibitors. Mol Cancer Res : MCR 2015;13:1465–77.
[18] Zandarashvili L, Langelier M-F, Velagapudi UK, Hancock MA, Steffen JD, Billur R, et al. Structural basis for allosteric PARP-1 retention on DNA breaks. Science 2020;368:eaax6367.
[19] Kondrashova O, Nguyen M, Shield-Artin K, Tinker AV, Teng NNH, Harrell MI, et al. Secondary somatic mutations restoring RAD51C and RAD51D associated with acquired resistance to the PARP inhibitor rucaparib in high-grade ovarian carcinoma. Cancer Discov 2017;7:984–98.

[20] Grellety T, Peyraud F, Sevenet N, Tredan O, Dohollou N, Barouk-Simonet E, et al. Dramatic response to PARP inhibition in a PALB2-mutated breast cancer: Moving beyond BRCA. Ann Oncol 2020;31:822–3.
[21] Pilie PG, Gay CM, Byers LA, O'Connor MJ, Yap TA. PARP inhibitors: Extending benefit beyond BRCA-mutant cancers. Clin Cancer Res 2019;25:3759–71.
[22] Yap TA, Plummer R, Azad NS, Helleday T. The DNA damaging revolution: PARP inhibitors and beyond. Am Soc Clin Oncol Educ Book 2019;39:185–95.
[23] Barber LJ, Sandhu S, Chen L, Campbell J, Kozarewa I, Fenwick K, et al. Secondary mutations in BRCA2 associated with clinical resistance to a PARP inhibitor. J Pathol 2013;229:422–9.
[24] Giudice E, Gentile M, Salutari V, Ricci C, Musacchio L, Carbone MV, et al. PARP inhibitors resistance: Mechanisms and perspectives. Cancers (Basel) 2022;14.
[25] Parsels LA, Engelke CG, Parsels J, Flanagan SA, Zhang Q, Tanska D, et al. Combinatorial efficacy of olaparib with radiation and ATR inhibitor requires PARP1 protein in homologous recombination-proficient pancreatic cancer. Mol Cancer Ther 2021;20:263–73.
[26] Tran Chau V, Liu W, Gerbe de Thore M, Meziani L, Mondini M, O'Connor MJ, et al. Differential therapeutic effects of PARP and ATR inhibition combined with radiotherapy in the treatment of subcutaneous versus orthotopic lung tumour models. Br J Cancer 2020;123:762–71.
[27] Soni A, Li F, Wang Y, Grabos M, Krieger LM, Chaudhary S, et al. Inhibition of Parp1 by BMN673 effectively sensitizes cells to radiotherapy by upsetting the balance of repair pathways processing DNA double-strand breaks. Mol Cancer Ther 2018;17:2206–16.
[28] Soni A, Lin X, Mladenov E, Mladenova V, Stuschke M, Iliakis G. BMN673 is a PARP inhibitor with unique radiosensitizing properties: Mechanisms and potential in radiation therapy. Cancers (Basel) 2022;14.
[29] Lesueur P, Chevalier F, El-Habr EA, Junier MP, Chneiweiss H, Castera L, et al. Radiosensitization effect of talazoparib, a parp inhibitor, on glioblastoma stem cells exposed to low and high linear energy transfer radiation. Sci Rep 2018;8:3664.
[30] DuRoss AN, Neufeld MJ, Landry MR, Rosch JG, Eaton CT, Sahay G, et al. Micellar formulation of talazoparib and buparlisib for enhanced DNA damage in breast cancer chemoradiotherapy. ACS Appl Mater Interfaces 2019;11:12342–56.
[31] Laird JH, Lok BH, Ma J, Bell A, de Stanchina E, Poirier JT, et al. Talazoparib is a potent radiosensitizer in small cell lung cancer cell lines and xenografts. Clin Cancer Res 2018;24:5143–52.
[32] Carter R, Cheraghchi-Bashi A, Westhorpe A, Yu S, Shanneik Y, Seraia E, et al. Identification of anticancer drugs to radiosensitise BRAF-wild-type and mutant colorectal cancer. Cancer Biol Med 2019;16:234–46.
[33] Magin S, Meher PK, Iliakis G. Nucleoside analogs radiosensitize G0 cells by activating DNA end resection and alternative end-joining. Radiat Res 2021;195:412–26.
[34] Magin S, Papaioannou M, Saha J, Staudt C, Iliakis GE. Inhibition of homologous recombination and promotion of mutagenic repair of DNA double-strand breaks underpins arabinoside-nucleoside analog-radiosensitization. Mol Cancer Ther 2015;14:1424–33.
[35] Feng W, Simpson DA, Cho J-E, Carvajal-Garcia J, Smith Chelsea M, Headley KM, et al. Marker-free quantification of repair pathway utilization at Cas9-induced double-strand breaks. Nucleic Acids Res 2021;49:5095–105.
[36] Mladenov E, Magin S, Soni A, Iliakis G. DNA double-strand-break repair in higher eukaryotes and its role in genomic instability and cancer: Cell cycle and proliferation-dependent regulation. Semin Cancer Biol 2016;37–38:51–64.
[37] Iliakis G, Mladenov E, Mladenova V. Necessities in the processing of DNA double strand breaks and their effects on genomic instability and cancer. Cancers 2019;11:1671.
[38] Mladenov E, Fan X, Dueva R, Soni A, Iliakis G. Radiation-dose-dependent functional synergisms between ATM, ATR and DNA-PKcs in checkpoint control and resection in G2-phase. Sci Rep 2019;9:8255.
[39] Mladenov E, Staudt C, Soni A, Murmann-Konda T, Siemann-Loekes M, Iliakis G. Strong suppression of gene conversion with increasing DNA double-strand break load delimited by 53BP1 and RAD52. Nucleic Acids Res 2020;48:1905–24.
[40] Iliakis G, Murmann T, Soni A. Alternative end-joining repair pathways are the ultimate backup for abrogated classical non-homologous end-joining and homologous recombination repair: Implications for the formation of chromosome translocations. Mutation Res/Genet Toxicol Environ Mutagenesis 2015;793:166–75.
[41] Schipler A, Iliakis G. DNA double-strand-break complexity levels and their possible contributions to the probability for error-prone processing and repair pathway choice. Nucleic Acids Res 2013;41:7589–605.
[42] Soni A, Siemann M, Grabos M, Murmann T, Pantelias GE, Iliakis G. Requirement for Parp-1 and DNA ligases 1 or 3 but not of Xrcc1 in chromosomal translocation formation by backup end joining. Nucleic Acids Res 2014;42:6380–92.
[43] Ceccaldi R, Rondinelli B, D'Andrea AD. Repair pathway choices and consequences at the double-strand break. Trends Cell Biol 2016;26:52–64.
[44] Wyatt DW, Feng W, Conlin MP, Yousefzadeh MJ, Roberts SA, Mieczkowski P, et al. Essential roles for polymerase theta-mediated end joining in the repair of chromosome breaks. Mol Cell 2016;63:662–73.
[45] Lee-Theilen M, Matthews AJ, Kelly D, Zheng S, Chaudhuri J. CtIP promotes microhomology-mediated alternative end joining during class-switch recombination. Nat Struct Mol Biol 2011;18:75–9.
[46] Truong LN, Li Y, Shi LZ, Hwang PY, He J, Wang H, et al. Microhomology-mediated End Joining and Homologous Recombination share the initial end resection step to repair DNA double-strand breaks in mammalian cells. PNAS 2013;110:7720–5.
[47] Xie A, Kwok A, Scully R. Role of mammalian Mre11 in classical and alternative nonhomologous end joining. Nat Struct Mol Biol 2009;16:814–8.
[48] Wang M, Wu W, Wu W, Rosidi B, Zhang L, Wang H, et al. PARP-1 and Ku compete for repair of DNA double strand breaks by distinct NHEJ pathways. Nucleic Acids Res 2006;34:6170–82.
[49] Ceccaldi R, Liu JC, Amunugama R, Hajdu I, Primack B, Petalcorin MIR, et al. Homologous-recombination-deficient tumours are dependent on Pol[thgr]-mediated repair. Nature 2015;518:258–62.
[50] Yu W, Lescale C, Babin L, Bedora-Faure M, Lenden-Hasse H, Baron L, et al. Repair of G1 induced DNA double-strand breaks in S-G2/M by alternative NHEJ. Nat Commun 2020;11:5239.
[51] Schrempf A, Slyskova J, Loizou JI. Targeting the DNA repair enzyme polymerase theta. Cancer Ther Trends Cancer 2021;7:98–111.
[52] Brambati A, Barry RM, Sfeir A. DNA polymerase theta (Poltheta) - an error-prone polymerase necessary for genome stability. Curr Opin Genet Dev 2020;60:119–26.
[53] Belan O, Sebald M, Adamowicz M, Anand R, Vancevska A, Neves J, et al. POLQ seals post-replicative ssDNA gaps to maintain genome stability in BRCA-deficient cancer cells. Mol Cell 2022;82:4664–4680.e9.
[54] Yi G, Sung Y, Kim C, Ra JS, Hirakawa H, Kato Takamitsu A, et al. DNA polymerase θ-mediated repair of high LET radiation-induced complex DNA double-strand breaks. Nucleic Acids Res 2023.
[55] Kumar RJ, Chao HX, Simpson DA, Feng W, Cho MG, Roberts VR, et al. Dual inhibition of DNA-PK and DNA polymerase theta overcomes radiation resistance induced by p53 deficiency. NAR Cancer 2020;2:zcaa038.
[56] Kuei CH, Lin HY, Lin MH, Lee HH, Lin CH, Lee WJ, et al. DNA polymerase theta repression enhances the docetaxel responsiveness in metastatic castration-resistant prostate cancer. Biochim Biophys Acta Mol basis Dis 2020;1866:165954.
[57] Lemee F, Bergoglio V, Fernandez-Vidal A, Machado-Silva A, Pillaire MJ, Bieth A, et al. DNA polymerase theta up-regulation is associated with poor survival in breast cancer, perturbs DNA replication, and promotes genetic instability. PNAS 2010;107:13390–5.
[58] Ronson GE, Starowicz K, Anthony EJ, Piberger AL, Clarke LC, Garvin AJ, et al. Mechanisms of synthetic lethality between BRCA1/2 and 53BP1 deficiencies and DNA polymerase theta targeting. Nat Commun 2023;14:7834.
[59] Sullivan-Reed K, Toma MM, Drzewiecka M, Nieborowska-Skorska M, Nejati R, Karami A, et al. Simultaneous targeting of DNA polymerase theta and PARP1 or RAD52 triggers dual synthetic lethality in homologous recombination-deficient leukemia cells. Mol Cancer Res : MCR 2023;21:1017–22.
[60] Zatreanu D, Robinson HMR, Alkhatib O, Boursier M, Finch H, Geo L, et al. Polθ inhibitors elicit BRCA-gene synthetic lethality and target PARP inhibitor resistance. Nat Commun 2021;12:3636.
[61] Zhou J, Gelot C, Pantelidou C, Li A, Yucel H, Davis RE, et al. A first-in-class polymerase theta inhibitor selectively targets homologous-recombination-deficient tumors. Nat Cancer 2021;2:598–610.
[62] Li F, Mladenov E, Sun Y, Soni A, Stuschke M, Timmermann B, et al. low CDK activity and enhanced degradation by APC/CCDH1 abolishes CtIP activity and Alt-EJ in quiescent cells. Cells 2023;12:1530.
[63] Kelso AA, Lopezcolorado FW, Bhargava R, Stark JM. Distinct roles of RAD52 and POLQ in chromosomal break repair and replication stress response. PLoS Genet 2019;15:e1008319.
[64] Gunn A, Stark JM. I-SceI-based assays to examine distinct repair outcomes of mammalian chromosomal double strand breaks. Methods Mol Biol (Clifton, NJ) 2012;920:379–91.
[65] Krieger LM, Mladenov E, Soni A, Demond M, Stuschke M, Iliakis G. Disruption of chromatin dynamics by hypotonic stress suppresses HR and shifts DSB processing to error-prone SSA. Int J Mol Sci 2021;22.
[66] Kinner A, Wu WQ, Staudt C, Iliakis G. gamma-H2AX in recognition and signaling of DNA double-strand breaks in the context of chromatin. Nucleic Acids Res 2008;36:5678–94.
[67] Soni A, Murmann-Konda T, Siemann-Loekes M, Pantelias GE, Iliakis G. Chromosome breaks generated by low doses of ionizing radiation in G2-phase are processed exclusively by gene conversion. DNA Repair (Amst) 2020;89:102828.
[68] Mladenov E, Fan X, Paul-Konietzko K, Soni A, Iliakis G. DNA-PKcs and ATM epistatically suppress DNA end resection and hyperactivation of ATR-dependent G2-checkpoint in S-phase irradiated cells. Sci Rep 2019;9:14597.
[69] Sartori AA, Lukas C, Coates J, Mistrik M, Fu S, Bartek J, et al. Human CtIP promotes DNA end resection. Nature 2007;450:509–14.
[70] Hopfner K-P, Karcher A, Craig L, Woo TT, Carney JP, Tainer JA. Structural biochemistry and interaction architecture of the dna double-strand break repair mre11 nuclease and rad50-atpase. Cell 2001;105:473–85.
[71] Stracker TH, Petrini JHJ. The MRE11 complex: Starting from the ends. Nat Rev Mol Cell Biol 2011;12:90–103.
[72] Luo Y, Cheng Y, Wu C, Ye H, Chen N, Zhang F, et al. Pharmacokinetics, safety, and antitumor activity of talazoparib monotherapy in Chinese patients with advanced solid tumors. Invest New Drugs 2023;41:503–11.
[73] Rodon Ahnert J, Tan DS, Garrido-Laguna I, Harb W, Bessudo A, Beck JT, et al. Avelumab or talazoparib in combination with binimetinib in metastatic pancreatic ductal adenocarcinoma: Dose-finding results from phase Ib of the JAVELIN PARP MEKi trial. ESMO Open 2023;8:101584.
[74] Wainberg ZA, Singh AS, Konecny GE, McCann KE, Hecht JR, Goldman J, et al. Preclinical and clinical trial results using talazoparib and low-dose chemotherapy. Clin Cancer Res 2023;29:40–9.
[75] Gruber JJ, Afghahi A, Timms K, DeWees A, Gross W, Aushev VN, et al. A phase II study of talazoparib monotherapy in patients with wild-type BRCA1 and BRCA2 with a mutation in other homologous recombination genes. Nat Cancer 2022;3:1181–91.
[76] Coquan E, Clarisse B, Lequesne J, Brachet PE, Nevière Z, Meriaux E, et al. TALASUR trial: A single arm phase II trial assessing efficacy and safety of

TALazoparib and Avelumab as maintenance therapy in platinum-Sensitive metastatic or locally advanced URothelial carcinoma. BMC Cancer 2022;22:1213.
[77] Agarwal N, Azad AA, Carles J, Fay AP, Matsubara N, Heinrich D, et al. Talazoparib plus enzalutamide in men with first-line metastatic castration-resistant prostate cancer (TALAPRO-2): a randomised, placebo-controlled, phase 3 trial. Lancet 2023;402:291–303.
[78] Higgins GS, Prevo R, Lee YF, Helleday T, Muschel RJ, Taylor S, et al. A small interfering RNA screen of genes involved in DNA repair identifies tumor-specific radiosensitization by POLQ knockdown. Cancer Res 2010;70:2984–93.
[79] Rodriguez-Berriguete G, Ranzani M, Prevo R, Puliyadi R, Machado N, Bolland HR, et al. Small-molecule poltheta inhibitors provide safe and effective tumor radiosensitization in preclinical models. Clin Cancer Res 2023;29:1631–42.
[80] Rao X, Xing B, Wu Z, Bin Y, Chen Y, Xu Y, et al. Targeting polymerase θ impairs tumorigenesis and enhances radiosensitivity in lung adenocarcinoma. Cancer Sci 2023;114:1943–57.
[81] Caron MC, Sharma AK, O'Sullivan J, Myler LR, Ferreira MT, Rodrigue A, et al. Poly (ADP-ribose) polymerase-1 antagonizes DNA resection at double-strand breaks. Nat Commun 2019;10:2954.
[82] Patterson-Fortin J, Bose A, Tsai WC, Grochala C, Nguyen H, Zhou J, et al. Targeting DNA repair with combined inhibition of NHEJ and MMEJ induces synthetic lethality in TP53-mutant cancers. Cancer Res 2022;82:3815–29.
[83] Krais JJ, Glass DJ, Chudoba I, Wang Y, Feng W, Simpson D, et al. Genetic separation of Brca1 functions reveal mutation-dependent Poltheta vulnerabilities. Nat Commun 2023;14:7714.